Article

Controllable Water-Triggered Degradation of PCL Solution-Blown Nanofibrous Webs Made Possible by Lipase Enzyme Entrapment

Fnu Asaduzzaman [ID] and Sonja Salmon *[ID]

Textile Engineering, Chemistry and Science, Wilson College of Textiles, North Carolina State University, 1020 Main Campus Drive, Raleigh, NC 27695-8301, USA; fasaduz@ncsu.edu
* Correspondence: sisalmon@ncsu.edu

Abstract: Polymers in nanofibrous forms offer new opportunities for achieving triggered polymer degradation, which is important for functional and environmental reasons. The polycaprolactone (PCL) nanofibrous nonwoven polymer webs developed in this work by solution blow spinning with entrapped enzymes were completely, rapidly and controllably degraded when triggered by exposure to water. Lipase (CALB) from *Candida antarctica* was successfully entrapped in the PCL webs via an enzyme-compatible water-in-oil emulsion in the PCL–chloroform spinning solution with added surfactant. Protein (enzyme) in the nanofibrous webs was detected by Fourier Transform Infrared Spectroscopy (FTIR), while time of flight-secondary ion mass spectroscopy (ToF-SIMS) and laser confocal microscopy indicated that enzymes were immobilized within solid fibers as well as within microbead structures distributed throughout the webs. Degradation studies of CALB-enzyme functionalized solution-blown nonwoven (EFSBN)-PCL webs at 40 °C or ambient temperature showed that EFSBN-PCL webs degraded rapidly when exposed to aqueous pH 8 buffer. Scanning electron microscopy (SEM) images of partially degraded webs showed that thinner fibers disappeared first, thus, controlling fiber dimensions could control degradation rates. Rapid degradation was attributed to the combination of nanofibrous web structure and the distribution of enzymes throughout the webs. CALB immobilized in the solid dry webs exhibited long storage stability at room temperature or when refrigerated, with around 60% catalytic activity being retained after 120 days compared to the initial activity. Dry storage stability at ambient conditions and rapid degradation upon exposure to water demonstrated that EFSBN-PCL could be used as fibers or binders in degradable textile or paper products, as components in packaging, for tissue engineering and for controlled-release drug or controlled-release industrial and consumer product applications.

Keywords: CALB; degradation; enzyme; immobilization; polycaprolactone; solution blow spinning

1. Introduction

Material biodegradability has garnered fresh attention for its role in environmental sustainability [1,2], leading to renewed interest in fully biodegradable materials that offer feasible alternatives to conventional polymers when recycling is not economically feasible or technically possible [3,4]. Especially for single-use, controlled-release or non-durable applications, biodegradable polymers are important alternatives to more common non-biodegradable plastics. Polycaprolactone (PCL) has excellent properties in this regard, including good biodegradability, compatibility with other polymers, good processibility that enables versatile fabrication of structures and forms, and it has a relatively low cost [5–7]. As a result, potential PCL applications are currently being examined for biodegradable packaging [8], controlled-release drug delivery [9], tissue engineering [10,11], and other biomaterial applications [12]. The Food and Drug Administration (FDA) has approved some PCL-containing products for use in humans because PCL is safely excreted from the body in the form of water-soluble fragments from its hydrolytic degradation

(PCL→6-hydroxycaproic acid→3-acetyl CoA→metabolism in the citric acid cycle→renal excretion) [12]. For instance, 'Capronor', a type of PCL rod, releases a progestin-like hormone for birth control purposes [13], 'Monocryl' sutures (copolymer of caprolactone and glycolide) are monofilament absorbable surgical sutures [14], and 'SynBiosys' drug release spheres are composed of multi-block copolymers of caprolactone lactide and ethyl glycol [15].

However, a limitation in the broader application of PCL for tissue scaffolds is its relatively slow degradation rate due to the five methylene repeating units that cause PCL to be more hydrophobic than other polyesters. The PCL degradation product (6-hydroxyhexanoic acid) is less acidic than degradation products from other polyesters, leading to less hydrolytic autocatalysis, and human body tissue implant sites generally lack indigenous enzymes capable of hydrolyzing PCL ester linkages [7,16]. Due to their hydrophobic and semi-crystalline nature, which slows the rate of hydration and subsequent hydrolytic cleavage, PCL-based polymer tissue scaffolds require up to 4 years to degrade completely [17]. PCL degradation starts in the amorphous regions, where water penetration causes hydrolysis of ester bonds, leading to chain scission and the formation of shorter chains, oligomers, and 6-hydroxyhexanoic acid [18]. The slow degradation restricts PCL use to applications like slow-release drug delivery devices and semi-durable implants.

PCL use could be expanded by regulating and accelerating its degradation rate by embedding hydrolytic enzymes within the PCL matrix. Enzymatic PCL degradation rate, which depends on the enzyme used, polymer composition, crystallinity, and physical form of the material, is generally complete after a few days [19]. For example, Shi et al. studied PCL film degradation in a *Candida antarctica* lipase buffer solution [20]. The PCL film (0.49 mm thickness) lost 87% of its initial weight after incubation at 37 °C for 3 days in the presence of 45 U/mL lipase solution. Ganesh et al. studied lipase-embedded PCL degradation where 1.6 and 6.5 wt% *Candida antarctica* lipase B (CALB) were encapsulated in PCL films [21]. The 6.5% CALB-loaded PCL film degraded completely within 24 h when incubated with shaking in pH 7.1 phosphate buffered solution at 37 °C, while 1.6 wt% CALB-loaded PCL films required 17 days. By measuring weight loss, these studies showed that enzyme-embedded PCL degradation is faster than pristine PCL degradation by hydrolysis; however they did not report residual enzyme activity. A triggered enzymatic degradation could enable CALB-embedded PCL matrices containing a therapeutic drug to undergo quick-release in medical applications. Including CALB directly in such applications would require further study and approval, though research shows that PEGylated versions of the enzyme would be possible that could potentially confer the necessary biocompatibility [22]. Meanwhile, rapid enzymatic degradation of PCL could be useful for making disposable packaging materials and controlled-release formulating agents for industrial and consumer products applications. However, more diverse and facile fabrication techniques are needed to modulate degradation times and end-use formats for enzyme-loaded PCL matrices.

Solution blow spinning (SBS) is a versatile continuous fiber processing method that produces polymeric micro-, submicron- and nanofibers with different properties depending on the polymers used [23,24]. During solution blow spinning, a polymer solution is injected into an annular die's core nozzle while high-pressure (speed) air flows through the concentric nozzle. The pressurized air stream causes the central polymer jet to stretch and bend while solvent evaporates which solidifies the polymer into nanofibrous nonwoven webs that can be collected on any form of collector [25,26]. An illustration and mechanism of a single needle solution blow spinning unit is shown in our previous work [27]. SBS produces fiber morphology that is similar to electrospinning [28,29], but at a much larger production rate and without high voltage requirements [30,31]. The higher production rate could make SBS processes viable for producing nanofibrous nonwovens at large scale. Several PCL-polymer blends were trialed in SBS processes [32–35], and SBS nanofibrous webs have been considered for packaging [36], controlled-release drug applications [37], filtration [38,39], tissue engineering [40], and other biomedical applications [41,42]. There-

fore, SBS holds promise as a potential technique for producing cost-effective fibrous PCL matrices with entrapped enzymes.

The goal of this work was to explore SBS fabrication for single-step enzyme co-immobilization in nanofibers from a combined polymer–organic solvent–enzyme solution. An organic solvent or polymer solution (continuous phase) with a small amount of aqueous phase (dispersed phase) forms a water-in-oil emulsion when using sodium bis(2-ethylhexyl)sulfosuccinate) (AOT) surfactant [43]. In this system, enzymes can retain their native structure inside the dispersed aqueous phase, even when the continuous (organic) phase is unfavorable for protein structure stability. Our investigation combined PCL, chloroform, AOT, and lipase from *Candida antarctica* (CALB). We hypothesized that CALB would remain active in the nanofiber webs produced from the PCL–chloroform-CALB triad by the mild SBS process; however, there were no prior reports of producing enzyme-loaded SBS fibers using this emulsion-based approach.

Herein, CALB entrapment in nanofibrous nonwoven webs by single-step PCL–chloroform solution blowing to produce unique enzyme-functionalized solution-blown nonwovens (EFSBNs) was demonstrated. EFSBN web physiochemical characteristics were analyzed, including web and fiber morphology, position and distribution of enzymes in the SBS fibers, enzyme activity, enzyme activity after dry web storage at different conditions, and enzymatic degradation of the PCL webs.

2. Materials and Methods

2.1. Materials

A liquid lipase product from *Candida* sp. (CALB), recombinantly expressed in *Aspergillus niger*, was purchased from Sigma-Aldrich (L3170) (Sigma-Aldrich, St. Louis, MO, USA) and used as supplied. Polycaprolactone pellets (M_n = 45,000 Da, specified by the supplier), p-nitrophenyl acetate, p-nitrophenyl, bis(2-ethylhexyl) sulfosuccinate sodium salt (AOT, also called docusate sodium salt), chloroform, and Tris-HCl were purchased from Sigma-Millipore (Hampton, NH, USA). Protein concentration in EFSBN was measured using a Pierce Rapid Gold BCA Protein Assay Kit (Catalog Numbers A53225, A53226, and A53227) from Thermo-Fisher Scientific (Waltham, MA, USA) together with the bovine serum albumin (BSA) standard provided in the kit.

2.2. SBN-PCL and EFSBN-PCL Web Production

Solution-blown nonwoven webs were produced using the same instrument and method described in our previous work [27]. PCL-based spinning solutions were prepared by dissolving PCL pellets (1.5 g) in AOT surfactant-loaded (1 mg AOT/mL solvent) chloroform (10 mL) with continuous (2 h) stirring (250 rpm). Liquid lipase (CALB) originating from *Candida antarctica* (75–1500 μL) added to a PCL-AOT-chloroform solution formed a water-in-oil emulsion after vortex mixing (2000 rpm, 1.5 min) and stirring (500 rpm, 3.5 min) to produce a visually uniform, turbid, translucent liquid that was stable during the time needed to perform solution blowing. After preparation, the emulsion liquids comprising PCL, chloroform, AOT surfactant, and CALB, were immediately subjected to solution blowing. Delivery of CALB dispersed in PCL solution (5 mL, 15 w/v%) to the inner spinning nozzle was controlled by a peristaltic pump, while compressed air (207 kPa) was blown through the outer nozzle. The polymer solution feed rate and air temperature were maintained at 0.5 mL/min and 40 °C, respectively. A collector was placed at a constant working distance (100 mm) from the needle tip. A schematic illustration of EFSBN-PCL webs production is presented in Figure 1. Enzyme-free PCL-only solution was also trialed with the same solution spinning conditions. The produced webs were stored at room temperature (~22 °C) or refrigerated (4 °C) until further analysis.
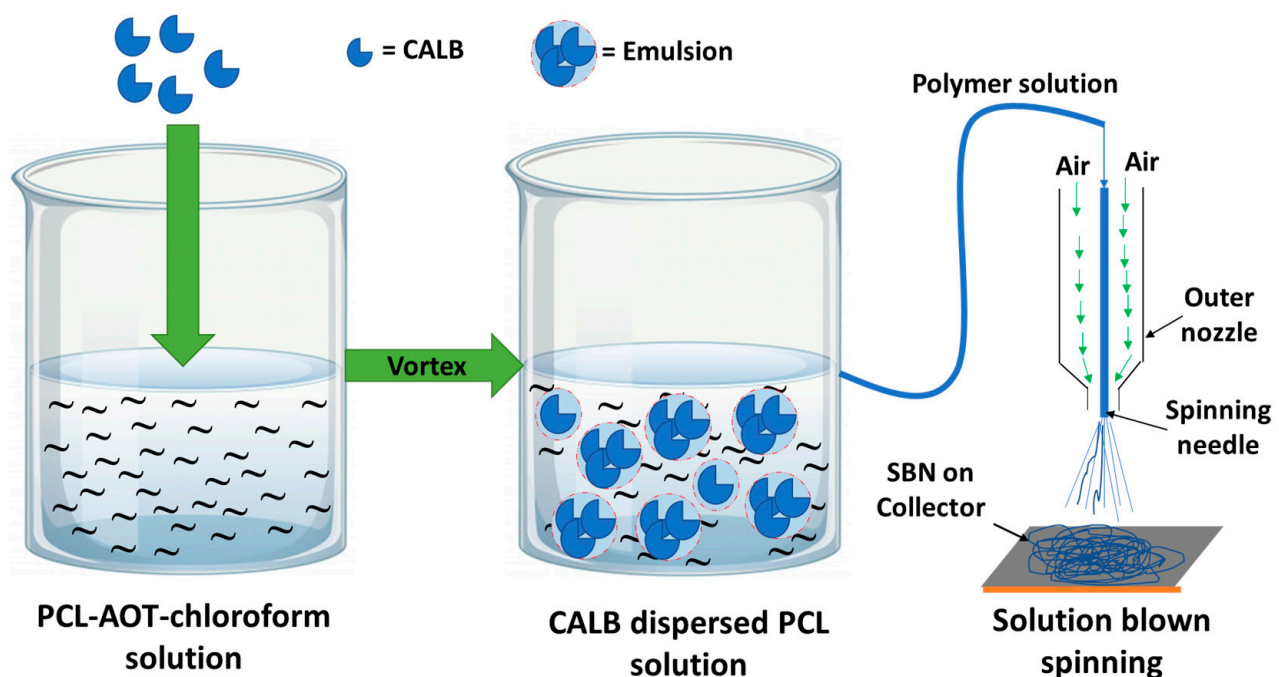
Figure 1. Schematic illustration of EFSBN-PCL preparation from AOT surfactant-loaded PCL–chloroform solution.

2.3. Protein Content and Immobilization Yield of EFSBN-PCL

The protein (enzyme) content in EFSBN-PCL was determined by modifying the Lowry assay method described in our previous work [27]. A Thermo Scientific Pierce™ Rapid Gold Bicinchoninic Acid (BCA) Protein Assay Kit was used for this analysis, where two molecules of BCA combine with one cuprous ion to form an orange-gold solution with an absorbance intensity at 480 nm that correlates to protein concentration. EFSBN-PCL webs were first incubated at 40 °C in tris buffer (pH 8.0, 0.1 M) for 120 min to degrade the webs entirely. Then, the degraded and dissolved web-containing solutions were used as unknown protein samples in the test protocol. Known concentrations of BSA protein (50–1500 µg/mL) were used to generate a standard curve and were tested along with the unknown protein samples. EFSBN-PCL protein content was calculated according to Equation (1), where C_{prot} is the measured protein concentration, V_{diss} is the redissolved volume, and m_{EFSBN} is the weight of the EFSBN sample before redissolution:

$$Protein\ content(\%) = \frac{C_{prot}(mg/ml) \times V_{diss}(ml) \times 100}{m_{EFSBN}(mg)} \tag{1}$$

EFSBN-PCL web immobilization yield was calculated using Equation (2), where $m_{1,prot}$ is the measured protein content in the solubilized EFSBN webs and $m_{2,prot}$ is the theoretical protein loading (amount of protein added) in the spinning solution.

$$Immobilization\ yield(\%) = \frac{m_{2,prot}(mg) \times 100}{m_{1,prot}(mg)} \tag{2}$$

2.4. Lipase Assay of Free and Immobilized CALB

The lipase activity of immobilized CALB was measured using a p-nitrophenyl acetate substrate-based assay method following a modification of the determination of carbonic anhydrase activity reported in previous work by Shen et al. [44]. The two-step protocol was adapted for microcentrifuge tube incubation. In the EFSBN-PCL web dissolution step, a suitable amount (approximately 10–15 mg, precisely weighed) of EFSBN-PCL web was placed into a 1.5 mL microcentrifuge vial and incubated with 1.20 mL Tris HCl buffer

(100 mM, pH 8.0) for 120 min at 40 °C. During incubation, EFSBN-PCL fibers were entirely dissolved and CALB was released into the buffer as free enzymes to produce a sample stock solution. Released enzymes behave like free enzymes when responding to lipase activity analysis. The p-nitrophenyl acetate substrate was first dissolved in ethanol to prepare a 100 mM substrate stock solution and kept at −4 °C for further assay measurements. Before each set of an assay, 100 mM p-NPAc was diluted with deionized water to a final concentration of 8 mM. In the incubation step, 75 µL of EFSBN-PCL redissolved stock solution and 400 µL Tris HCl buffer (100 mM, pH 8.0) were mixed and preincubated for 5 min. For free CALB activity, the free CALB liquid enzyme sample was first diluted (dilution factor 10,000) in 100 mM Tris buffer (pH 8.0); then, 475 µL of the dilution was added to a 1500 µL microcentrifuge tube and pre-incubated for 5 min at 45 °C. Then, 25 µL of 8 mM p-NPAc substrate solution was added to the free and immobilized CALB solutions and mixed thoroughly by gentle manual mixing. The final solution (total volume 500 µL) was incubated for 30 min at 45 °C. Active CALB catalyzes the hydrolysis of p-NPAc. After incubation, the reaction was stopped by placing microcentrifuge tubes into ice water. Absorbance measurements of the assay solutions determine the concentration of p-nitrophenol (p-NP), the yellow-colored product of p-NPAc hydrolysis, with an absorbance maximum of 405 nm. Three replicates of each sample were measured. The blank control was made by maintaining the same procedure except adding an equivalent amount of SBN-PCL (neat PCL web) instead of EFSBN-PCL. All solutions were kept in the same conditions throughout the assay process. A p-NP standard curve was created by plotting absorbance versus known concentrations of p-NP (5–50 µg/mL) (Figure S1). The micromoles of p-NP equivalents liberated were determined by using the standard curve. One unit (U) of lipase activity is defined as the amount of enzyme that catalyzes the release of 1.0 µmole of p-NP per min from the p-NPAc substrate at 40 °C in the presence of 100 mM pH 8.0 Tris-HCl buffer. A sample calculation of the lipase activity of free CALB and released EFSBN CALB is shown in Supplementary Material (Supplementary S1).

The lipase assay of the free liquid enzyme upon dilution was calculated using Equation (3) to obtain the volumetric activity and then using Equation (4) to obtain the mass-based specific enzyme activity, where $n_{p\text{-}NP}$ is the p-NP equivalent release, T is the incubation time, V_A and $V_{1,E}$ are the volume of total assay and used enzyme, respectively.

$$\frac{U}{ml} = \frac{n_{p-NP}(\mu mole) \times V_A(ml) \times dilution}{T(min) x V_{1,E}(ml)} \tag{3}$$

$$\frac{U}{mg_{protein}} = \frac{\frac{U}{ml}}{\frac{mg \ of \ protein}{ml \ of \ liquid \ CALB}} \tag{4}$$

The lipase assay of immobilized CALB per mg of the EFSBN-PCL webs protein was calculated using Equation (5), where $m_{3,prot}$ is the EFSBN's protein used in the assay and $V_{2,E}$ is the volume of redissolved EFSBN enzyme used in the assay.

$$U/mg_{EFSBNprotein} = \frac{n_{p-NP}(\mu mole) \times V_A(ml)}{T(min) \times m_{3,prot}(mg) \times V_{2,E}(ml)} \tag{5}$$

The relative activity of immobilized CALB was calculated as a percentage of the free lipase activity according to Equation (6):

$$Relative \ activity(\%) = \frac{Activity \ of \ immobilized \ lipase \times 100}{Activity \ of \ free \ lipase} \tag{6}$$

2.5. FTIR Spectroscopy Analysis of SBN-PCL and EFSBN-PCL

The presence of enzyme protein in the EFSBN-PCL was characterized by Fourier-transform infrared spectroscopy (FTIR) (iS50, ThermoFisher Scientific, Waltham, MA, USA) with a built-in diamond crystal Attenuated Total Reflection sampling head. Spectra were

collected for dried SBN-PCL and EFSBN-PCL webs at room temperature from 500 to 4000 cm^{-1} with 64 scans and 4 cm^{-1} resolution. All specimens were stored in a desiccator for two days before measurement to minimize moisture in the samples.

2.6. Enzyme Distribution in EFSBN-PCL by Confocal Microscopy

CALB was conjugated to fluorescein isothiocyanate (FITC) following the "large-scale conjugation" procedure described in the Sigma Fluoro-tag-FITC conjugation kit. After dispersing FITC-tag-CALB in PCL-AOT-chloroform solution, solution blown webs were produced, as described in Section 2.2. The resulting 0.32 wt% FITC-tag-CALB EFSBN-PCL webs were mounted on a glass slide under a No. 1.5 coverslip supported by clay spacers and imaged by a Zeiss LSM 880 laser scanning confocal microscope using a 488 nm excitation laser to detect the FITC signal. The z-series images were collected using a 20× dry objective with NA = 0.8 and 2 μm intervals. The z-series were further processed using Imaris 9.9 software (Bitplane, Zurich, Switzerland) to remove the background signal. Results show the location of CALB in EFSBN-PCL webs.

2.7. Surface Analysis Using ToF-SIMS

Surface analysis of EFSBN-PCL was performed using a time of flight-secondary ions mass spectroscopy (ToF-SIMS) (TOF SIMS V, ION TOF, Inc. Chestnut Ridge, NY, USA) instrument equipped with a Bi_n^{m+} (n = 1–5, m = 1, 2) liquid metal ion gun, Cs^+ sputtering gun, and electron flood gun for charge compensation. Both the Bi and Cs ion columns were oriented at 45° with respect to the sample surface normal. The analysis chamber pressure was maintained below 5.0×10^{-9} mbar to avoid contamination of the surfaces to be analyzed. In this study's high-lateral-resolution mass spectral images, a Burst Alignment setting of 25 keV Bi^{3+} ion beam was used to raster in a pixel region of 256 by 256 pixels. The negative secondary ion mass spectra obtained were calibrated using C^-, O^-, OH^-, CN^-, respectively. The positive secondary ion mass spectra were calibrated using C^+, $C_2H_3^+$, $C_3H_5^+$, $C_4H_7^+$.

2.8. EFSBN-PCL Degradation Analysis

Degradation studies of EFSBN-PCL webs were carried out using a batch process. SBN-PCL and EFSBN-PCL webs (~15 mg) were placed in 1500 μL microcentrifuge tubes containing 1000 μL Tris-HCl buffer solution (100 mM, pH 8.0). Incubations were performed with manual shaking (every 5 min intervals) in a dry bath incubator (Isotemp, Fisher Scientific) at 40 °C. All tubes were removed from the incubator every 15 min to take a visual picture and then placed in the incubator. The whole incubation process time was 60 min. Degradation studies of EFSBN-PCL webs at room temperature incubation were also observed in comparison to SBL-PCL webs and original PCL beads. PCL beads, SBN-PCL webs, and EFSBN-PCL webs (~30 mg) were immersed in microcentrifuge (2000 μL) tubes containing Tris-HCl buffer (1500 μL). For the PCL beads and SBN-PCL webs, free CALB was added to the buffer. The microcentrifuge tubes were then placed in tube holders at room temperature (~22 °C) for 4 h, and a picture was taken for visual comparison. For morphological analysis of degraded webs, fibers were removed from microcentrifuge tubes after 30 min incubation, dried, and stored for SEM analysis.

2.9. Morphological Analysis of SBN-PCL, EFSBN-PCL, and Degraded EFSBN-PCL Using SEM

Morphologies of SBN-PCL and EFSBN-PCL samples were investigated using field-emission scanning electron microscopy (FESEM) (FEI Verios 460L, FEI Company, Hillsboro, OR, USA) with an accelerating voltage of 500 V and a current of 2 pA. The morphology of EFSBN-PCL degraded webs was also observed using this instrument. Images were analyzed using ImageJ software (National Institutes of Health, Bethesda, MD, USA) to measure fiber diameters as an average of at least 100 measurements on each SEM micrograph.

2.10. Storage Stability of Free and Immobilized CALB-EFSBN-PCL

Storage stability of immobilized CALB and liquid-free CALB was evaluated by a modified method of Pereira et al. [45]. The EFSBN-PCL webs were kept in a zip-closure plastic bag, stored at room temperature (~22 °C), and refrigerated (4 °C). The as-supplied free liquid CALB and free CALB diluted (0.1 μL/mL) in Tris buffer (0.1 M, pH 8.0) were also stored at room temperature (~22 °C). After storage for 0–120 days, sample residual activities were determined using the p-NPAc spectrophotometric assay described above. Residual activity was calculated using Equation (7).

$$Relative\ residual\ activity(\%) = \frac{Measured\ activity\ of\ stored\ sample \times 100}{Initial\ sample\ activity} \quad (7)$$

3. Results and Discussion

3.1. SBN-PCL and EFSBN-PCL Preparation by Solution Spinning Process

The first step in producing EFSBN-PCL webs was to establish solution blow spinning parameters for producing benchmark SBN-PCL webs. Solution spinning trials were conducted using PCL pellets dissolved in surfactant-loaded (1 mg AOT/mL solvent) chloroform. Appropriate solution spinning conditions for producing SBN-PCL fibrous webs were determined to be 0.5 mL/min solution throughput, 207 kPa air pressure, 40 °C air temperature, 45 kDa molecular weight, 15 w/v% polymer solution, and 100 mm die to collector distance (DCD). The higher-molecular-weight (80 kDa) PCL solution clogged the spinning needle because a higher degree of polymerization (DP) causes more polymer chain entanglement and higher viscosity [46]. High solution throughput and low air pressure had a similar effect on fiber formation, where these conditions did not provide enough driving force to attenuate the polymer solution and ultimately failed to complete the necessary solvent evaporation. Once the solution spinning process conditions were selected for polymer-only solutions, the same spinning conditions were used for enzyme-loaded polymer solutions.

For EFSBN-PCL production, liquid CALB enzyme (0.75–15 v/v%) was dispersed in AOT surfactant loaded (1 mg AOT/mL solvent) PCL polymer solution (15 w/v%) and then immediately processed by solution blow spinning. Fiber formation depended on maintaining a stable aqueous phase in the water-in-oil emulsion polymer solution. For 0.75–7.5 v/v% CALB in polymer solutions, all solution that passed through the needle was converted to EFSBN-PCL webs, whereas for the 11.2 v/v% CALB in polymer solution, along with fiber production, a viscous mass accumulated beneath the spinning needle because the higher amount of water phase caused emulsion instability (Figure S2). With even higher enzyme loading (15 v/v% CALB in polymer solution), the spinning solution was not able to form fiber at all because of even more instability of the emulsion due to the higher amount of water present. Images showing the microscopic appearance of emulsion spinning solutions, containing dispersed phase droplets with diameters in the range of about 1–10 μm, and additional images of solution blown webs are included in Supplementary Material (Supplementary S2).

3.2. Enzyme Loading and Immobilization Yield of EFSBN-PCL

When used inside a degradable packaging material, the level of enzyme loading is expected to influence degradation time. To test this, a range of different CALB (0.53 to 1.92 wt%)-loaded EFSBN-PCL webs were prepared. Percent protein content and immobilization yields in solid webs are shown in Figure 2 for different protein (enzyme) loading levels in the polymer spinning solutions. "Protein loading" refers to the amount of protein initially added to the spinning solution before solution blowing, and "protein content" refers to the amount of protein detected in the final webs. The measurement of "immobilization yield" indicates how much enzyme added to the polymer solution was retained after solution blowing.
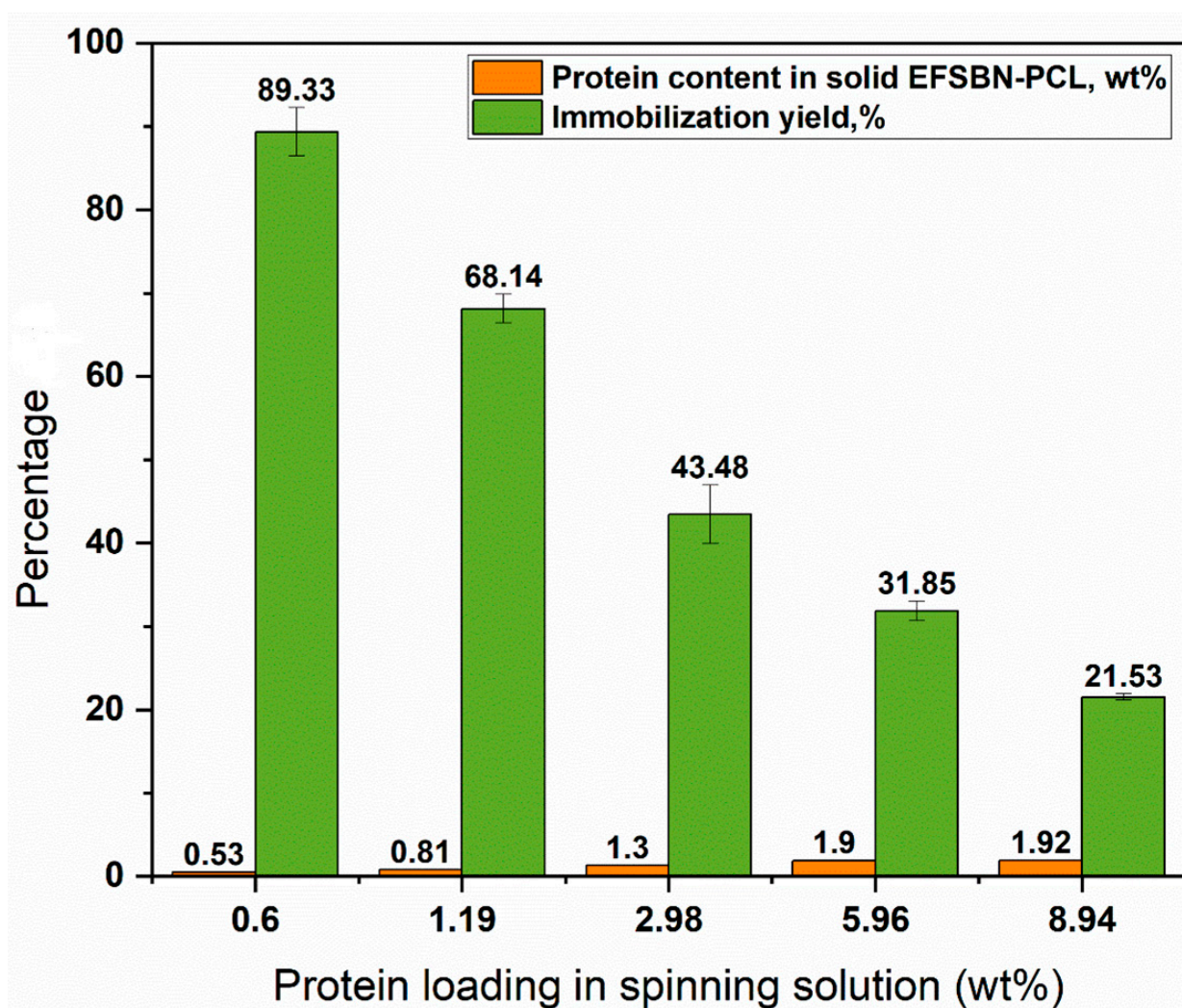
Figure 2. Immobilization yield of EFSBN-PCL and retained protein in the solid EFSBN-PCL webs with different enzyme loading in the spinning solution.

At low enzyme loading, immobilization yields had a higher value which decreased with increasing CALB loading in the spinning solution. This indicates that at low concentrations, it was possible to form a stable water-in-oil emulsion that could entrap most of the enzyme in the PCL nanofibers. However, the immobilization yield was only around 20% for 8.94 (wt%) protein loading in the spinning solution, which could be caused by instability of the emulsion (due to high water phase) or inability to dry all solvent during the solution blown process (resulting a viscous mass on collector observed underneath the spinning needle (Figure S2B). Another explanation for the less than 100% immobilization yields may be that some enzyme aerosolized and was blown away by the air stream [25]. Additionally, there may have been an artifact error in the Rapid BCA protein determination technique because the control sample had no PCL molecules, whereas the protein content sample contained some degraded PCL. Further work would be needed to clarify the specific cause(s) for the decrease in immobilization yield with increasing enzyme loading.

3.3. FTIR, ToF-SIMS and Laser Confocal Microscopy Analysis

FTIR was used to confirm the presence of CALB in the solution blown nanofiber webs (Figure 3). Infrared absorbance of PCL exhibited a main peak at 1725 and 1170 cm^{-1} due to C=O stretching and C-O-C stretching, respectively [47,48]. The N-H stretching peak of amide A from enzyme protein overlaps with O-H stretching from water, resulting a broad peak at 3100–3500 cm^{-1} [49]. Some bound water molecules are associated with the

enzyme structure [50], while additional water may be present from using a water-in-oil emulsion spinning solution to entrap enzymes inside individual fibers of the nanofibrous webs. Due to the low protein content (1.3% in the EFSBN-PCL webs), the characteristic amide I (1650 cm^{-1}) and amide II (1550 cm^{-1}) peaks of peptide bonds [51] are very small in EFSBN-PCL. However, the amide I peak intensity increased when a background correction using SBN-PCL webs was performed. Dry enzyme-free SBN-PCL webs do not exhibit peaks in this region. These results are consistent with reports where FTIR analysis confirmed lipase entrapment inside a polymer matrix by observing similar peaks [52].
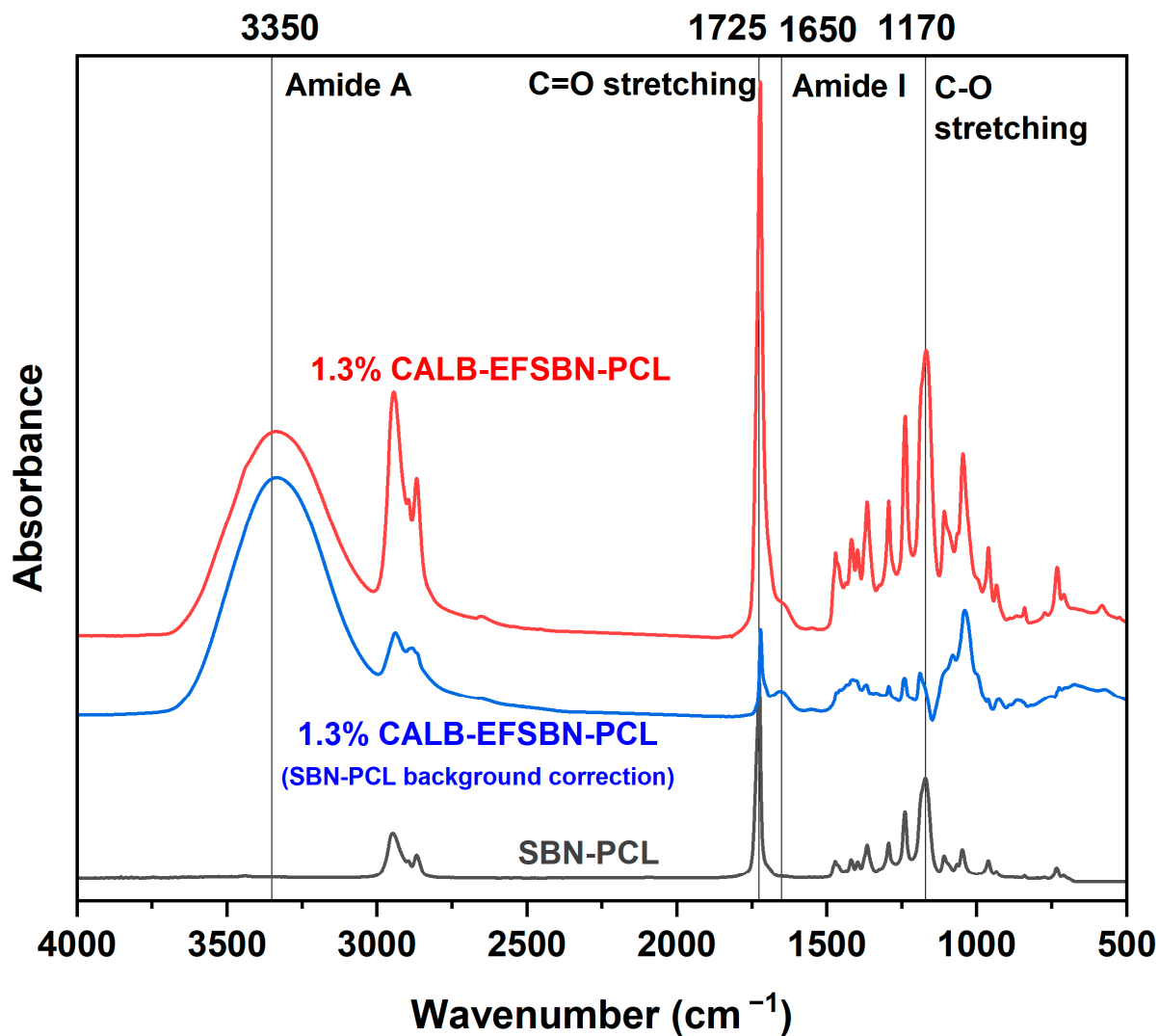

Figure 3. FTIR spectrum of SBN-PCL and CALB-EFSBN-PCL webs with normal air background correction (red) and SBN-PCL web background correction (blue).

ToF-SIMS spectra and distribution maps revealed the distribution and position of immobilized lipase. High lateral resolution mass spectral maps of SBN-PCL webs, 0.53 wt% CALB-EFSBN-PCL and 1.30 wt% CALB-EFSBN-PCL webs, are shown in Figure S8, Figure S9 and Figure S10, respectively. The negative ions (CN$^-$ and CNO$^-$) and total ions ratio of these three samples are shown in Figure S11. The absence of significant nitrogen peak intensities for EFSBN-PCL indicates that these nanofibers did not have enough protein molecules on the surface for detection because ToF-SIMS is limited to detecting ion fragments within 1–2 nm depth of the surface of a specimen. Therefore, for low enzyme-loaded EFSBN-PCL webs, the ToF-SIMS results support that most enzymes are inside the nanofibers or under a PCL layer rather than at the surface.

CALB distribution in EFSBN-PCL webs was observed by entrapping a fluorescent dye-tagged CALB into PCL webs, using fluorescein isothiocyanate (FITC) as the dye tag. FITC-tagged CALB entrapped inside PCL webs by solution blow spinning was analyzed by laser scanning confocal microscopy. Images of webs with 0.32 wt% entrapped FITC-labeled CALB are shown in Figure 4. These results illustrate that CALB distribution in EFSBN-PCL was not homogeneous at a microscopic level. The microscopic appearance is consistent with an aqueous liquid enzyme solution forming a water-in-oil emulsion in the PCL-AOT-chloroform solution, and this emulsion morphology was preserved after solution blowing. Enzymes remained together in aggregates in the dried PCL webs. Although the appearance is not homogeneous, nevertheless, solution blowing of enzyme-loaded PCL solutions was successful as an entrapment process for enzymes.
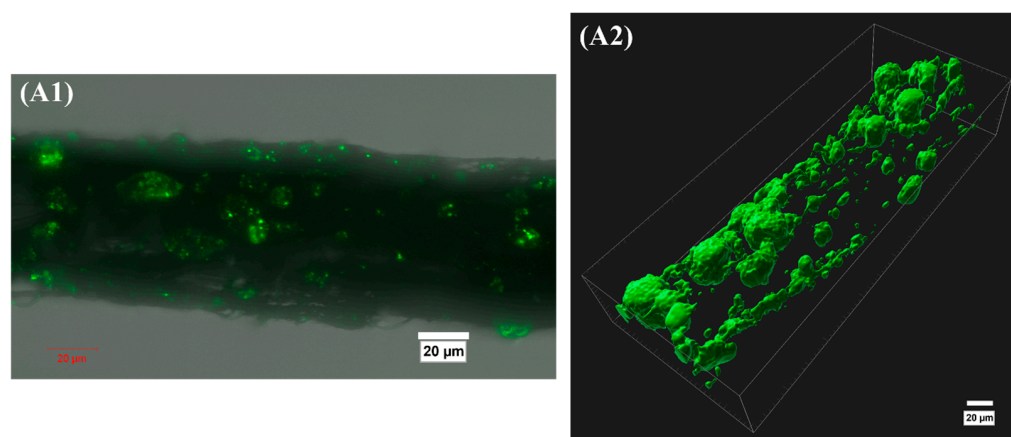

Figure 4. Laser scanning confocal microscopy images of the distribution of FITC-tagged CALB (0.32 wt%) entrapped in EFSBN-PCL webs: (**A1**) raw image and (**A2**) z-series image. Green represents the quantity of enzyme distribution throughout the web.

3.4. Enzymatic Degradation of EFSBN-PCL Webs

Controlled degradation is a useful property in material design and applications. PCL has excellent properties for controlled release and other transient applications due to the susceptibility of its ester bonds to hydrolysis, but the hydrolysis rate may be too slow for systems that require short lifetimes [21]. Depolymerization of PCL produces caprolactone (the cyclic monomer) or 6-hydroxyhexanoic acid (the ring opened form) and their low molecular weight oligomers, which are soluble in water [18]. Approaches that could accelerate PCL degradation rate include nanofabrication approaches that create materials with high surface area and exposure to hydrolytic enzymes as degradation catalysts. Entrapping CALB inside solution-blown PCL nanofibrous nonwoven webs meets both the requirement for high surface area and directly distributes enzymes throughout the webs during material fabrication. As a result, extremely fast enzymatic degradation of EFSBN-PCL was observed (Figure 5) across a range of protein loadings in the webs incubated at 40 °C in pH 8 buffer. The high (1.90 and 1.92 wt%) CALB-loaded EFSBN-PCL webs degraded so rapidly that within 15 min, these webs were entirely degraded to soluble components, with no visible solids remaining. Since the CALB-free SBN-PCL did not visibly degrade within the same time period, the combined effects of the small diameter nanofibers (and corresponding high surface area) that exposed exterior surfaces of PCL to the aqueous buffer plus the presence of hydrolytic CALB trapped inside the fibers of the web as hydrophilic aggregates were responsible for the rapid nanofiber degradation. The degradation rate depended on the level of enzyme loading, and even the lowest (0.53 wt%) CALB-loaded web degraded much faster (within 60 min) than was reported for 6.5 wt% and 1.6 wt% CALB embedded PCL films (incubated at 37 °C in 20 mM phosphate buffer at pH 7.10 with 200 rpm shaking), which required 24 h and 17 days, respectively, to achieve complete degradation [21]. A trendline showing the relationship between CALB enzyme

loading and approximate EFSBN-PCL web degradation time is shown in Supplementary Material (Supplementary S3, Figure S14).

CALB-containing EFSBN-PCL webs (Figure 6C) also exhibited more rapid degradation at pH 8 and ambient temperature (~22 °C) compared to an equivalent mass of PCL-beads (Figure 6E) or no-enzyme SBN-PCL webs (Figure 6D) that were incubated in buffer solutions containing free CALB at a similar protein amount as contained in the EFSBN-PCL web. Table 1 summarizes the incubation conditions and total weight loss of PCL webs and beads after 240 min enzymatic degradation in a Tris-HCl buffer (pH 8.0, 100 mM) at ambient conditions (~22 °C). As shown in Figure 6 and Table 1, neither SBN-PCL nor PCL-pellet was visibly degraded at room temperature after 240 min incubation, and no weight loss was detected. The faster degradation of EFSBN-PCL was achieved because CALB-catalyzed degradation could occur both at the exterior surface (from released free enzyme) and inside or near the nanofibers (due to entrapped enzyme). In contrast, free CALB added to the buffer could only act on SBN-PCL nanofiber surfaces, leading to somewhat slower polymer degradation to soluble products, though complete degradation was also achieved due to the high nanofiber surface area, which itself is a benefit of solution blown nanofibers for accelerated degradation. In contrast, the degradation of PCL-beads was very slow compared with nanofibers. A similar mass of PCL-bead incubated in a similar amount of free CALB in buffer showed only 7.2% weight loss (Figure 6E), and treatment with even five times more free CALB resulted in only 6.9% weight loss (Figure 6F), after 240 min room temperature incubation. The dramatic difference in surface area can explain the degradation behavior of nanofibers versus beads. Based on an average fiber diameter of 220 ± 73 nm, the estimated superficial surface area of EFSBN-PCL webs was about 11,000 times higher than that of the PCL beads, for the same mass of nanofibers and beads (Supplementary S4). The large SBN surface area exposes more ester linkages as hydrolytic reaction sites on the nanofibers, resulting in fast degradation, even at ambient temperature. Rapid degradation at ambient temperature implies that EFSBN-PCL could be used in degradable packaging, wipes or sheets, tissue engineering, or drug release applications.

3.5. Morphology Analysis of EFSBN-PCL and Partially Degraded EFSBN-PCL

The morphologies of SBN-PCL, EFSBN-PCL and partially degraded webs prepared with different CALB loadings were observed by scanning electron microscopy (Figure 7). Before incubation, the morphology of each sample was characteristic of a nonwoven structure with a distribution of micro- and nanofibers forming the web. SBN-PCL web fibers were more uniform than EFSBN-PCL webs. Occasional "beads" formed from droplets of incompletely attenuated PCL were observed in SBN-PCL (Figure S12), and the frequency of these beads trapped within the fibrous web increased with increased enzyme loading in EFSBN-PCL. Changes in fiber diameter and web morphology appearance also occurred as enzyme loading increased. Higher enzyme-loaded webs had comparatively larger diameters and larger diameter variations due to clustering and "welding" between fibers (Figure S13). The observation by SEM of beads with diameters in the 5–20 μm range for 0.53 wt% CALB-EFSBN-PCL webs (Figure S12) and by optical microscopy of dispersed phase droplets having diameters in the 1–10 μm range in the spinning liquid emulsion (Figure S5) is consistent with the fluorescence distribution shown in Figure 4 for FITC-tagged CALB loaded at 0.32 wt% in EFSBN-PCL webs, indicating that most of the CALB was localized in the beads. Since more beading and fiber-to-fiber adhesion was observed with increasing protein content in the webs, these irregularities in fiber diameter and emergence of fiber clustering and beading are attributed to an increased resistance by the spinning solution to being stretched when the amount of aqueous phase in the water-in-oil emulsion of the PCL–AOT–chloroform–CALB spinning solution increased. Less stretching leads to larger fiber diameters and slower solvent evaporation, which leads to larger bead formation from agglomerated unstretched microdroplets and results in stickier fibers and adhesion between fibers that causes clustering. Although the magnified images emphasize the microscopic irregularity, in fact the microbeads are distributed throughout

the webs, creating "pockets" of enzyme activity that are effective at rapidly degrading the webs upon exposure to water. Additionally, notably, the beads appear intact with smooth surfaces (Figure S12), not cracked or ruptured, implying that aqueous phase microdroplets containing enzymes were surrounded and entrapped by the PCL polymer solution during solution blowing.
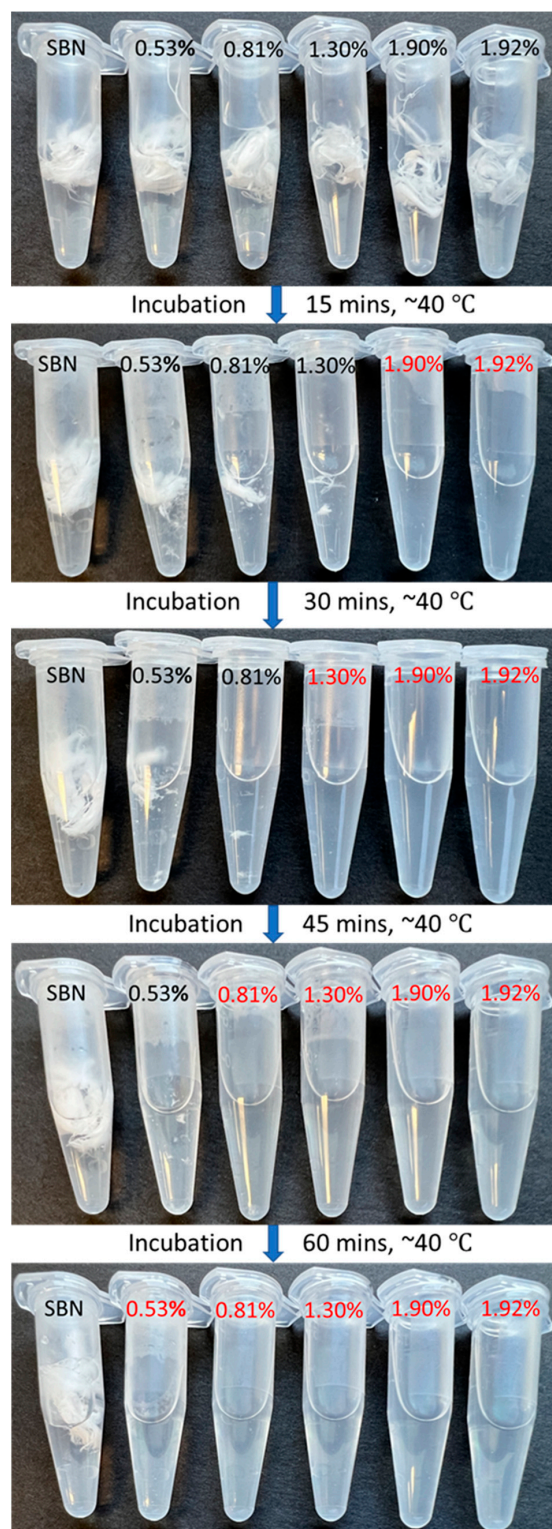

Figure 5. Enzymatic degradation of EFSBN-PCL in tris buffer (100 mM, 8.0 pH) incubation at 40 °C.
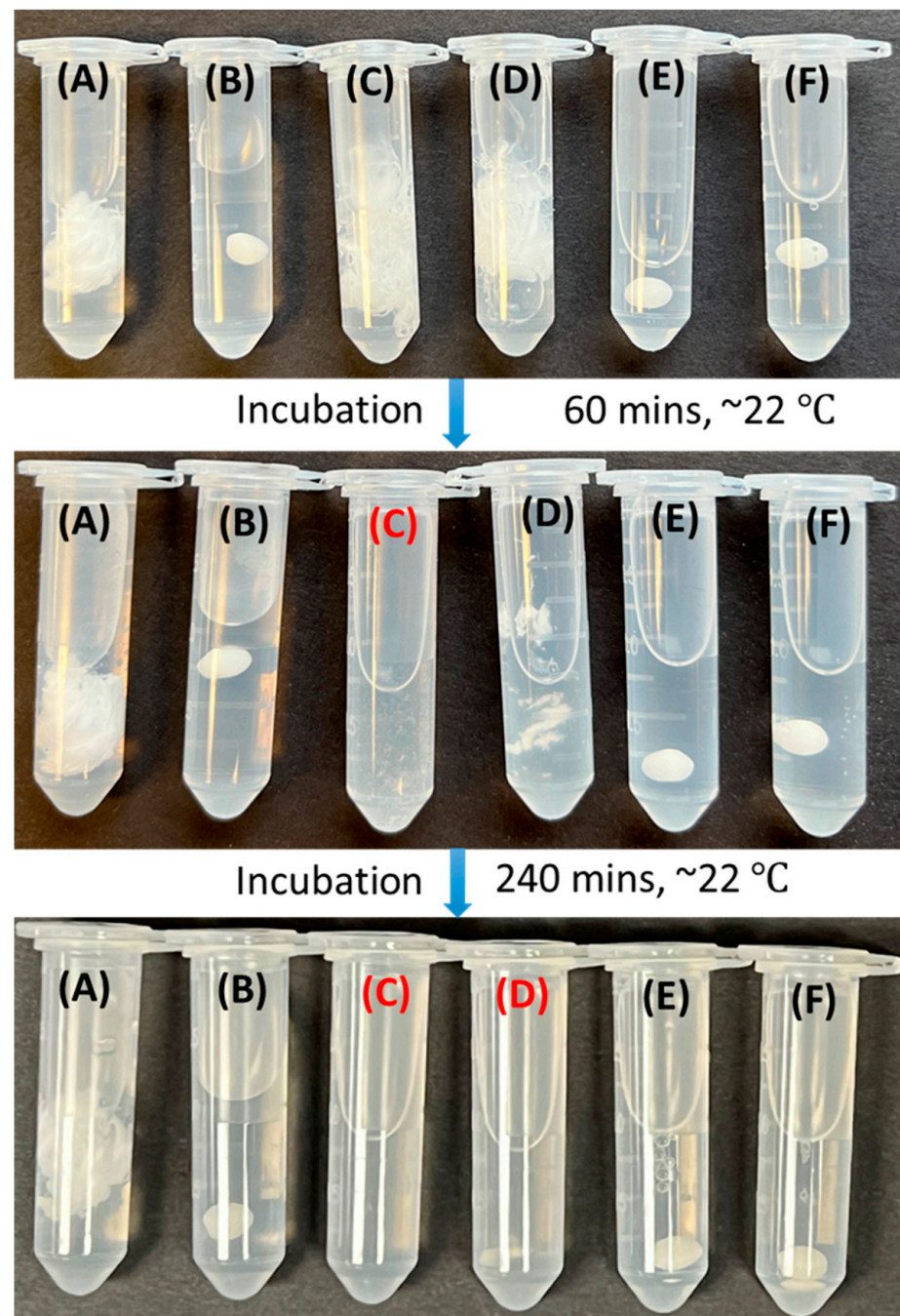
Figure 6. Enzymatic degradation of SBN-PCL, EFSBN-PCL and PCL bead in a Tris-HCl buffer (pH 8.0, 100 mM) at ambient conditions (~22 °C) for samples: (**A**) SBN-PCL in buffer, (**B**) PCL-bead in buffer, (**C**) 1.30 wt% CALB-EFSBN-PCL in buffer (0.238 mg protein CALB loading/mL buffer), (**D**) SBN-PCL in free CALB (50-times dilution) in buffer (0.232 mg protein CALB loading/mL buffer), (**E**) PCL-bead in free CALB (50-times dilution) in buffer (0.232 mg protein CALB loading/mL buffer), and (**F**) PCL-bead in free CALB (10-times dilution) in buffer (1.192 mg protein CALB loading/mL buffer). Top image shows the initial appearance of the samples; middle image shows the samples after 1 h incubation, where sample (**C**) is almost fully degraded; and, bottom image shows that both samples (**C**) and (**D**) are fully degraded after a total of 4 h incubation.

Table 1. Weight loss of SBN-PCL, EFSBN-PCL and PCL bead after 240 min enzymatic degration in a Tris-HCl buffer (pH 8.0, 100 mM) at ambient conditions (~22 °C).

Sample	Incubation Medium	Equivalent Protein, mg Protein Loading/mL Buffer	Weight Loss, %
SBN-PCL	Buffer-only	0	0
PCL bead	Buffer-only	0	0
1.30% CALB -EFSBN-PCL	Buffer-only	0.238	100
SBN-PCL	Free CALB in buffer	0.232	100
PCL bead	Free CALB in buffer	0.232	7.2
PCL bead	Free CALB in buffer	1.192	6.9
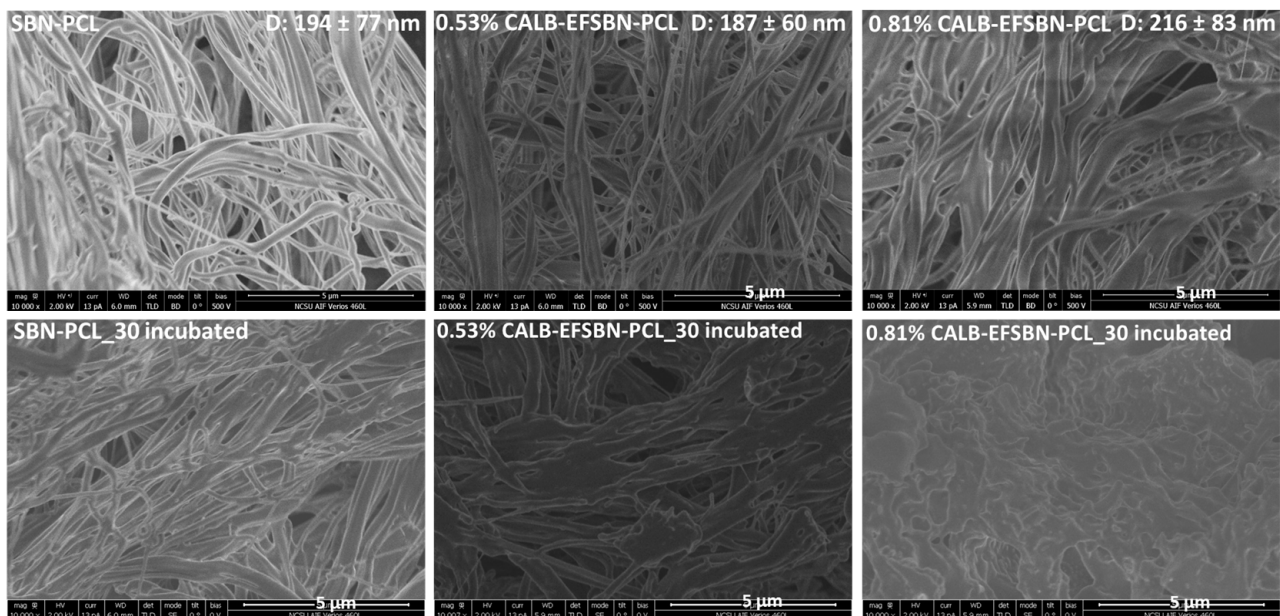
Figure 7. SEM micrograph (10,000× magnification) of SBN-PCL and EFSBN-PCL webs before and after incubation in Tris-HCl buffer (pH 8.0, 100 mM) at 40 °C for 30 min. Average fiber diameters (D) of non-incubated SBN-PCL and EFSBN-PCL nanofibers are shown in the respective micrographs.

SEM micrographs of residual web solids after incubation in a buffer (Figure 7) give insight into the degradation mechanism. Whereas discrete fibers were still observed in the SBN-PLC sample after incubation, the fine fiber structure in partially degraded EFSBN-PCL webs disappeared, and, at high enzyme loading, the individual fiber morphology was completely gone, leaving an irregular solid mass. Since PCL is a hydrophobic polymer, as it degrades, the remaining polymer would tend to aggregate in clusters to exclude water, which matches the appearance of the observed residual solids. The SEM micrographs indicate that thinner nanofibers degraded more quickly, and this phenomenon occurred throughout the whole web, leading to the appearance of an overall homogeneous degradation. Additionally, during incubation, CALB released from the degradation of thinner nanofibers could become available to help degrade larger fibers from the outside in. Therefore, deliberately varying fiber sizes and combining fibers of different sizes with different levels of enzyme loading, including combinations of fibers with and without enzyme, could be useful strategies for developing products with controlled degradation times.

3.6. Biocatalytic Activity of Free and Immobilized CALB

CALB-loaded EFSBN-PCL webs were entirely degradable in pH 8 buffer after incubation at 40 °C, which released CALB into the buffer as a free enzyme that could respond to lipase activity analysis. Released CALB activity was calculated relative to the amount of protein detected in the solid webs. Then, the percent relative activity of EFSBN webs was calculated from the ratio of degraded EFSBN-PCL webs activity compared to the activity of an equivalent amount of free enzyme protein. The lipase activities of CALB-EFSBN-PCL webs relative to their measured protein content are presented in Figure 8. The EFSBN-PCL showed around 50% retained catalytic activity, indicating that the enzyme delivered through the solution-blowing nozzle still retained a useful level of activity in the final solid web products. This level of catalytic activity also indicated that at least some immobilized CALB retained its functional structure in the PCL–chloroform solution or was able to recover its functional structure when the webs were exposed to buffer solution. Other factors, such as vigorous vortex mixing during emulsion preparation, together with solvent exposure and the stress of solution blowing, could lead to protein denaturation, which would explain the loss of hydrolytic activity. Nevertheless, the amount of retained activity was comparable to the activity of a free *Candida rugosa* lipase that was incubated in an anhydrous chloroform solvent [53]. The substantial retained activity of CALB indicates that the solution-blown spinning process is a promising technique for entrapping lipase inside PCL carriers from a PCL-organic solvent solution.
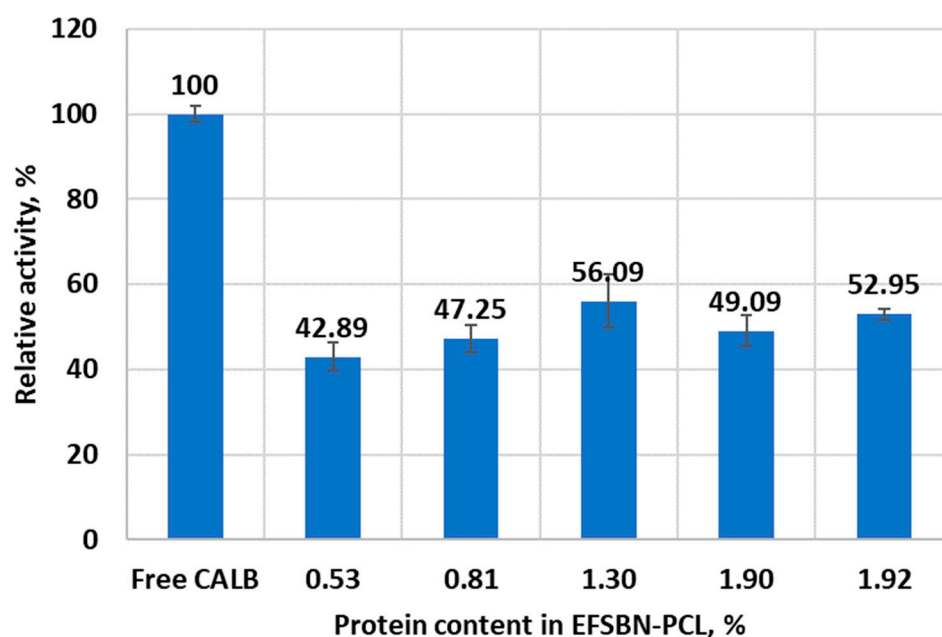

Figure 8. Relative catalytic activity of CALB-EFSBN-PCL webs with varying protein content in the solid webs.

3.7. Storage Stability of Free CALB and CALB-EFSBN-PCL

The room temperature storage stabilities of immobilized CALB, free CALB (as supplied), and free CALB diluted in pH 8 buffer were compared. Relative retained activities at different storage times are presented in Figure 9A. Immobilized CALB showed similar storage stability to the as-supplied liquid CALB, whereas buffer-diluted CALB retained less than 20% activity after 120 days. The commercial liquid CALB product may have a stabilizer that loses effectiveness after dilution in buffer, which could explain the rapid decrease in enzyme activity for the diluted sample. The similar (or even better) retained activity outcome for CALB in EFSBN-PCL webs compared to stabilized commercial liquid CALB showed that the dry EFSBN-PCL webs tolerate ambient storage conditions for a long time. The good stability is attributed to the dry webs stabilizing the entrapped enzyme molecular

structures and preventing them from unfolding and losing activity. A similar observation has been reported for *Candida rugosa* lipase immobilized on amino-functionalized magnetic supports, where immobilized lipase maintained more than 80% of its initial activity during a 30-day storage period, while the free lipase lost all activity under the same conditions [54]. The high level of retained activity indicates that EFSBN-PCL can be stored at dry conditions in a convenient solid form for long periods of time and will still have active enzymes inside that become active when exposed to water, causing rapid triggered degradation due to the high surface area of the SBN. EFSBN-PCL could be made in many different shapes and sizes, and in mixtures, composites or layers together with other materials, leading to many useful applications.
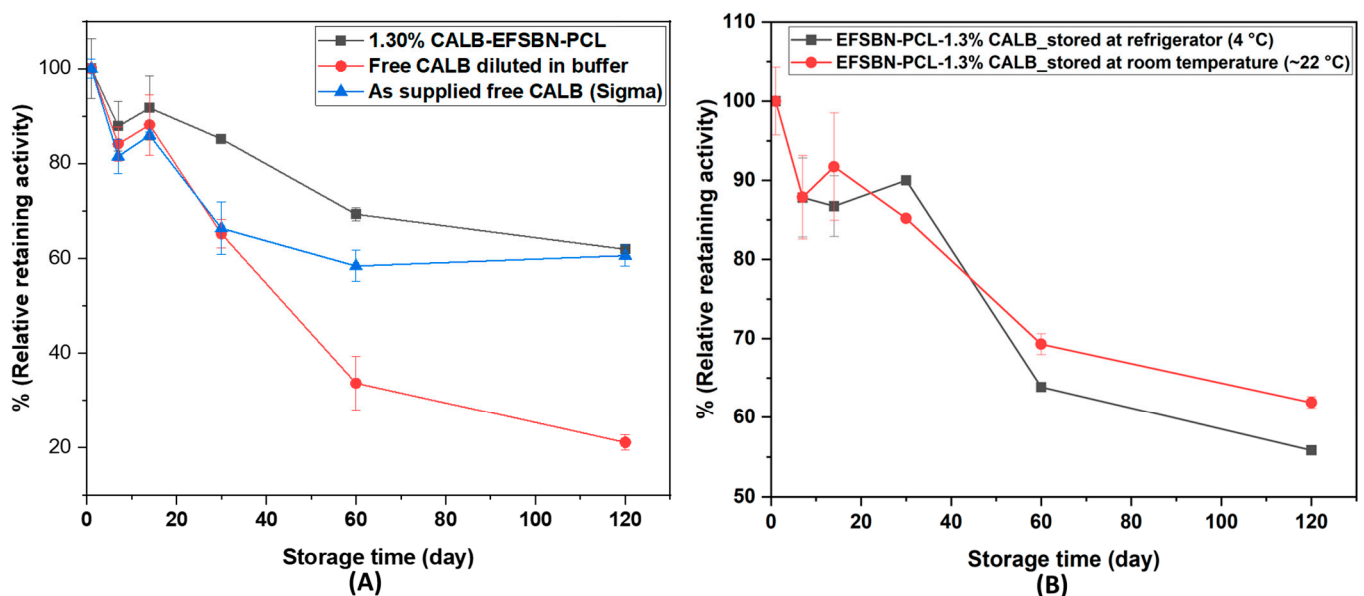

Figure 9. (**A**) Ambient (~22 °C) storage stability of supplied free CALB, diluted free CALB (0.1 μL/mL) in Tris HCl buffer (pH = 8.0, 100 mM) and 1.30 wt% CALB-EFSBN-PCL solid webs and (**B**) Storage stability (retaining activity with time) of 1.3 wt% CALB-EFSBN-PCL webs at ambient and refrigerator temperatures.

Figure 9B shows CALB-loaded EFSBN-PCL web storage stability at ambient and refrigerated temperatures. The results show that immobilized CALB was stable for a long time in dry PCL webs. After PCL degradation and solubilization in the buffer, enzyme released from both webs showed around 60% of their initial activity after 120 days. This means CALB immobilized in EFSBN-PCL webs could be conveniently stored at ambient temperature, as an alternative to refrigerator storage. Futhermore, these tests revealed that CALB-containing dry solid EFSBN-PCL webs remained intact at ambient or refrigerated temperature without degrading. The storage stability results imply that CALB enzymes retain their structure in dry EFSBN-PCL but do not degrade PCL webs because CALB is not active without moisture [16]. When moisture is present to trigger the reaction, CALB becomes active on wet EFSBN-PCL webs and catalyzes the degradation of ester linkages of the PCL polymer chains. Thus, EFSBN-PCL webs could be used as enzyme-degradable packaging material at ambient conditions.

4. Conclusions

CALB enzyme-functionalized solution-blown nonwoven polycaprolactone (CALB-EFSBN-PCL) nanofibrous webs were successfully prepared from water-in-oil emulsions of PCL–chloroform–CALB by a single-step solution blowing technique. Although the same solution blow spinning process parameters, including air pressure, solution flow rate, and die-to-collector distance, were used for PCL-only and CALB-loaded PCL webs,

the morphologies and fiber diameters in EFSBN-PCL webs varied depending on CALB loading. SEM micrographs revealed more irregular, clustered and beaded nonwoven fiber structures in EFSBN-PCL compared to SBN-PCL. FTIR spectra and Lowry protein assay results confirmed the presence of protein in the nanofibrous webs. ToF-SIMS surface characterization and laser confocal microscopy imaging indicated that immobilized enzymes were mainly located inside the fibers or within unattenuated microbeads that were distributed throughout the webs. Substantial enzyme activity was detected in EFSBN-PCL webs after the solution-blowing process and after storage at ambient dry conditions. CALB released from EFSBN-PCL webs exhibited about 50% activity compared to an equivalent amount of free CALB. EFSBN-PCL webs were stable under dry conditions, retaining more than 60% activity after 120 days for both ambient and refrigerated dry storage, but degraded rapidly when exposed to aqueous buffer due to the presence of hydrolytic enzymes entrapped within the high surface area nanofiber and microbead structures of the webs. Higher enzyme loading led to faster degradation, and complete degradation was achieved within <15 min (40 °C) or < 120 min (22 °C). Successful enzyme entrapment in dry EFSBN-PCL webs with water-triggered rapid enzymatic degradation make these materials useful for applications in packaging materials, wipes and disposable sheets, for tissue engineering, and for controlled-release drug or controlled-release industrial and consumer products applications.

Supplementary Materials: The following supporting information can be downloaded at: https://www.mdpi.com/article/10.3390/fib11060049/s1; Supplementary S1. Lipase assay calculation of free CALB and redissolved CALB-EFSBN-PCL, Figure S1: Calibration curve for p-nitrophenol (p-NP) concentration measured at 405 nm; Supplementary S2. Morphology of solution blown webs with and without enzyme, Figure S2: (A) SBN-PCL and (B) CALB-EFSBN-PCL webs on collectors produced using chloroform solvent; Figure S3: Exemplary preparation of a nominal 0.7 v/v% CALB in 15 w/v% PCL in chloroform-AOT solvent emulsion; Figure S4: Optical microscopic images of 15 w/v% PCL in chloroform-AOT solvent; Figure S5: Optical microscopic images of a nominal 0.7 v/v% CALB in 15 w/v% PCL in chloroform-AOT solvent emulsion; Figure S6: Optical microscopic images of the emulsion shown in Figure S5; Figure S7: Optical microscopic images of a nominal 1.5 v/v% CALB in 15 w/v% PCL in chloroform-AOT solvent emulsion; Figure S8: ToF-SIMS high lateral resolution mass spectral maps (analysis area 100×100 μm^2) of SBN-PCL webs; Figure S9: ToF-SIMS high lateral resolution mass spectral maps (analysis area 100×100 μm^2) of 0.53 wt% CALB-EFSBN-PCL webs; Figure S10: ToF-SIMS high lateral resolution mass spectral maps (analysis area 100×100 μm^2) of 1.30 wt% CALB-EFSBN-PCL webs; Figure S11: (CN+CNO)/total ion count graph of SBN-PCL, 0.53 wt% CALB-EFSBN-PCL and 1.30 wt% CALB-EFSBN-PCL webs; Figure S12: SEM micrograph ($2000\times$ magnification) of SBN-PCL webs and CALB-EFSBN-PCL webs with varying enzyme loading; Figure S13: SEM micrograph ($10,000\times$ magnification) of SBN-PCL webs and CALB-EFSBN-PCL webs with varying enzyme loading; Supplementary S3. Relationship between degradation time and enzyme loading in EFSBN-PCL webs, Figure S14: Relationship between approximate degradation time and level of CALB enzyme loading in EFSBN-PCL webs; Supplementary S4. Surface area (estimated) calculation of EFSBN-PCL and PCL bead.

Author Contributions: Conceptualization, F.A. and S.S.; methodology, F.A.; validation, F.A. and S.S.; formal analysis, F.A.; investigation, F.A.; resources, S.S.; data curation, F.A.; writing—original draft preparation, F.A.; writing—review and editing, S.S.; visualization, F.A. and S.S.; supervision, S.S.; project administration, F.A. and S.S.; funding acquisition, S.S. All authors have read and agreed to the published version of the manuscript.

Data Availability Statement: The article, the Supplementary Material and the Ph.D. Dissertation by F.A. titled "Enzyme Functionalized Solution Blown Nonwovens" (2022), available at https://www.lib.ncsu.edu/resolver/1840.20/40206, accessed on 22 May 2023 include the research data pertaining to this study.

Conflicts of Interest: The authors declare no conflict of interest. The funders had no role in the design of the study; in the collection, analyses, or interpretation of data; in the writing of the manuscript; or in the decision to publish the results.

References

1. Milovanovic, S.; Hollermann, G.; Errenst, C.; Pajnik, J.; Frerich, S.; Kroll, S.; Rezwan, K.; Ivanovic, J. Supercritical CO2 Impregnation of PLA/PCL Films with Natural Substances for Bacterial Growth Control in Food Packaging. *Food Res. Int.* **2018**, *107*, 486–495. [CrossRef] [PubMed]
2. Tawakkal, I.S.M.A.; Cran, M.J.; Miltz, J.; Bigger, S.W. A Review of Poly(Lactic Acid)-Based Materials for Antimicrobial Packaging. *J. Food Sci.* **2014**, *79*, R1477–R1490. [CrossRef] [PubMed]
3. Naser, A.Z.; Deiab, I.; Darras, B.M. Poly(Lactic Acid) (PLA) and Polyhydroxyalkanoates (PHAs), Green Alternatives to Petroleum-Based Plastics: A Review. *RSC Adv.* **2021**, *11*, 17151–17196. [CrossRef] [PubMed]
4. Egan, J.; Salmon, S. Strategies and Progress in Synthetic Textile Fiber Biodegradability. *SN Appl. Sci.* **2022**, *4*, 22. [CrossRef]
5. Hadj-Hamou, A.S.; Metref, F.; Yahiaoui, F. Thermal Stability and Decomposition Kinetic Studies of Antimicrobial PCL/Nanoclay Packaging Films. *Polym. Bull.* **2017**, *74*, 3833–3853. [CrossRef]
6. Khan, R.A.; Beck, S.; Dussault, D.; Salmieri, S.; Bouchard, J.; Lacroix, M. Mechanical and Barrier Properties of Nanocrystalline Cellulose Reinforced Poly (Caprolactone) Composites: Effect of Gamma Radiation. *J. Appl. Polym. Sci.* **2013**, *110*, 3038–3046. [CrossRef]
7. Englert, C.; Brendel, J.C.; Majdanski, T.C.; Yildirim, T.; Schubert, S.; Gottschaldt, M.; Windhab, N.; Schubert, U.S. Pharmapolymers in the 21st Century: Synthetic Polymers in Drug Delivery Applications. *Prog. Polym. Sci.* **2018**, *87*, 107–164. [CrossRef]
8. Cabedo, L.; Feijoo, J.L.; Villanueva, M.P.; Lagarón, J.M.; Giménez, E. Optimization of Biodegradable Nanocomposites Based on APLA/PCL Blends for Food Packaging Applications. *Macromol. Symp.* **2006**, *233*, 191–197. [CrossRef]
9. Grossen, P.; Witzigmann, D.; Sieber, S.; Huwyler, J. PEG-PCL-Based Nanomedicines: A Biodegradable Drug Delivery System and Its Application. *J. Control. Release* **2017**, *260*, 46–60. [CrossRef]
10. Siddiqui, N.; Asawa, S.; Birru, B.; Baadhe, R.; Rao, S. PCL-Based Composite Scaffold Matrices for Tissue Engineering Applications. *Mol. Biotechnol.* **2018**, *60*, 506–532. [CrossRef]
11. Pant, H.R.; Neupane, M.P.; Pant, B.; Panthi, G.; Oh, H.-J.; Lee, M.H.; Kim, H.Y. Fabrication of Highly Porous Poly (ε-Caprolactone) Fibers for Novel Tissue Scaffold via Water-Bath Electrospinning. *Colloids Surf. B Biointerfaces* **2011**, *88*, 587–592. [CrossRef] [PubMed]
12. Malikmmammadov, E.; Tanir, T.E.; Kiziltay, A.; Hasirci, V.; Hasirci, N. PCL and PCL-Based Materials in Biomedical Applications. *J. Biomater. Sci. Polym. Ed.* **2018**, *29*, 863–893. [CrossRef] [PubMed]
13. Sivasankaran, S.; Jonnalagadda, S. Advances in Controlled Release Hormonal Technologies for Contraception: A Review of Existing Devices, Underlying Mechanisms, and Future Directions. *J. Control. Release* **2021**, *330*, 797–811. [CrossRef] [PubMed]
14. Müller, D.A.; Snedeker, J.G.; Meyer, D.C. Two-Month Longitudinal Study of Mechanical Properties of Absorbable Sutures Used in Orthopedic Surgery. *J. Orthop. Surg. Res.* **2016**, *11*, 111. [CrossRef]
15. Neves, A.; Godina, R.; Azevedo, S.G.; Matias, J.C.O. A Comprehensive Review of Industrial Symbiosis. *J. Clean. Prod.* **2020**, *247*, 119113. [CrossRef]
16. Ganesh, M.; Gross, R.A. Embedded Enzymatic Biomaterial Degradation: Flow Conditions & Relative Humidity. *Polymer* **2012**, *53*, 3454–3461. [CrossRef]
17. Pitt, C.G.; Chasalow, F.I.; Hibionada, Y.M.; Klimas, D.M.; Schindler, A. Aliphatic Polyesters. I. The Degradation of Poly(ε-Caprolactone) in vivo. *J. Appl. Polym. Sci.* **1981**, *26*, 3779–3787. [CrossRef]
18. Bosworth, L.A.; Downes, S. Physicochemical Characterisation of Degrading Polycaprolactone Scaffolds. *Polym. Degrad. Stab.* **2010**, *95*, 2269–2276. [CrossRef]
19. Li, F.; Yu, D.; Lin, X.; Liu, D.; Xia, H.; Chen, S. Biodegradation of Poly(ε-Caprolactone) (PCL) by a New Penicillium Oxalicum Strain DSYD05-1. *World J. Microbiol. Biotechnol.* **2012**, *28*, 2929–2935. [CrossRef]
20. Shi, K.; Jing, J.; Song, L.; Su, T.; Wang, Z. Enzymatic Hydrolysis of Polyester: Degradation of Poly(ε-Caprolactone) by Candida Antarctica Lipase and Fusarium Solani Cutinase. *Int. J. Biol. Macromol.* **2020**, *144*, 183–189. [CrossRef]
21. Ganesh, M.; Dave, R.N.; Amoreaux, W.L.; Gross, R. a Embedded Enzymatic Biomaterial Degradation. *Macromolecules* **2009**, *42*, 6836. [CrossRef]
22. Gupta, V.; Bhavanasi, S.; Quadir, M.; Singh, K.; Ghosh, G.; Vasamreddy, K.; Ghosh, A.; Siahaan, T.J.; Banerjee, S.; Banerjee, S.K. Protein PEGylation for Cancer Therapy: Bench to Bedside. *J. Cell Commun. Signal.* **2019**, *13*, 319–330. [CrossRef] [PubMed]
23. Zhang, J.; Kitayama, H.; Gotoh, Y. High Strength Ultrafine Cellulose Fibers Generated by Solution Blow Spinning. *Eur. Polym. J.* **2020**, *125*, 109513. [CrossRef]

24. Li, X.; Teng, S.; Xu, X.; Wang, H.; Dong, F.; Zhuang, X.; Cheng, B. Solution Blowing of Polyacrylonitrile Nanofiber Mats Containing Fluoropolymer for Protective Applications. *Fibers Polym.* **2018**, *19*, 775–781. [CrossRef]

25. Kolbasov, A.; Sinha-Ray, S.; Joijode, A.; Hassan, M.A.; Brown, D.; Maze, B.; Pourdeyhimi, B.; Yarin, A.L. Industrial-Scale Solution Blowing of Soy Protein Nanofibers. *Ind. Eng. Chem. Res.* **2016**, *55*, 323–333. [CrossRef]

26. Sinha-Ray, S.; Sinha-Ray, S.; Yarin, A.L.; Pourdeyhimi, B. Theoretical and Experimental Investigation of Physical Mechanisms Responsible for Polymer Nanofiber Formation in Solution Blowing. *Polymer* **2015**, *56*, 452–463. [CrossRef]

27. Asaduzzaman, F.; Salmon, S. Protease Immobilization in Solution-Blown Poly(Ethylene Oxide) Nanofibrous Nonwoven Webs. *ACS Appl. Eng. Mater.* **2023**, *1*, 447–457. [CrossRef]

28. Kumar, A.; Sinha-Ray, S. A Review on Biopolymer-Based Fibers via Electrospinning and Solution Blowing and Their Applications. *Fibers* **2018**, *6*, 45. [CrossRef]

29. Pant, B.; Park, M.; Park, S.J. Drug Delivery Applications of Core-Sheath Nanofibers Prepared by Coaxial Electrospinning: A Review. *Pharmaceutics* **2019**, *11*, 305. [CrossRef]

30. Miranda, K.W.E.; Mattoso, L.H.C.; Bresolin, J.D.; Hubinger, S.Z.; Medeiros, E.S.; de Oliveira, J.E. Polystyrene Bioactive Nanofibers Using Orange Oil as an Ecofriendly Solvent. *J. Appl. Polym. Sci.* **2019**, *136*, 47337. [CrossRef]

31. Uyar, T.; Besenbacher, F. Electrospinning of Uniform Polystyrene Fibers: The Effect of Solvent Conductivity. *Polymer* **2008**, *49*, 5336–5343. [CrossRef]

32. Cao, Y.; Shen, C.; Yang, Z.; Cai, Z.; Deng, Z.; Wu, D. Polycaprolactone/Polyvinyl Pyrrolidone Nanofibers Developed by Solution Blow Spinning for Encapsulation of Chlorogenic Acid. *Food Qual. Saf.* **2022**, *6*, fyac014. [CrossRef]

33. Li, R.; Li, Z.; Yang, R.; Yin, X.; Lv, J.; Zhu, L.; Yang, R. Polycaprolactone/Poly(L-Lactic Acid) Composite Micro/Nanofibrous Membrane Prepared through Solution Blow Spinning for Oil Adsorption. *Mater. Chem. Phys.* **2020**, *241*, 122338. [CrossRef]

34. Lorente, M.A.; Corral, A.; González-Benito, J. PCL/Collagen Blends Prepared by Solution Blow Spinning as Potential Materials for Skin Regeneration. *J. Appl. Polym. Sci.* **2021**, *138*, 50493. [CrossRef]

35. Lv, J.; Yin, X.; Li, R.; Chen, J.; Lin, Q.; Zhu, L. Superhydrophobic PCL/PS Composite Nanofibrous Membranes Prepared through Solution Blow Spinning with an Airbrush for Oil Adsorption. *Polym. Eng. Sci.* **2019**, *59*, E171–E181. [CrossRef]

36. Shen, C.; Cao, Y.; Rao, J.; Zou, Y.; Zhang, H.; Wu, D.; Chen, K. Application of Solution Blow Spinning to Rapidly Fabricate Natamycin-Loaded Gelatin/Zein/Polyurethane Antimicrobial Nanofibers for Food Packaging. *Food Packag. Shelf Life* **2021**, *29*, 100721. [CrossRef]

37. Ferreira, K.N.; Oliveira, R.R.; Castellano, L.R.C.; Bonan, P.R.F.; Carvalho, O.V.; Pena, L.; Souza, J.R.; Oliveira, J.E.; Medeiros, E.S. Controlled Release and Antiviral Activity of Acyclovir-Loaded PLA/PEG Nanofibers Produced by Solution Blow Spinning. *Biomater. Adv.* **2022**, *136*, 212785. [CrossRef]

38. Liu, Y.; Zhang, G.; Zhuang, X.; Li, S.; Shi, L.; Kang, W.; Cheng, B.; Xu, X. Solution Blown Nylon 6 Nanofibrous Membrane as Scaffold for Nanofiltration. *Polymers* **2019**, *11*, 364. [CrossRef]

39. Wang, Y.; Chao, G.; Li, X.; Dong, F.; Zhuang, X.; Shi, L.; Cheng, B.; Xu, X. Hierarchical Fibrous Microfiltration Membranes by Self-Assembling DBS Nanofibrils in Solution-Blown Nanofibers. *Soft Matter* **2018**, *14*, 8879–8882. [CrossRef]

40. Popkov, A.V.; Kulbakin, D.E.; Popkov, D.A.; Gorbach, E.N.; Kononovich, N.A.; Danilenko, N.V.; Stankevich, K.S.; Choynzonov, E.L.; Zheravin, A.A.; Khlusov, I.A.; et al. Solution Blow Spinning of PLLA/Hydroxyapatite Composite Scaffolds for Bone Tissue Engineering. *Biomed. Mater.* **2021**, *16*, 055005. [CrossRef]

41. Behrens, A.M.; Casey, B.J.; Sikorski, M.J.; Wu, K.L.; Tutak, W.; Sandler, A.D.; Kofinas, P. In Situ Deposition of PLGA Nanofibers via Solution Blow Spinning. *ACS Macro Lett.* **2014**, *3*, 249–254. [CrossRef] [PubMed]

42. Tomecka, E.; Wojasinski, M.; Jastrzebska, E.; Chudy, M.; Ciach, T.; Brzozka, Z. Poly(L-Lactic Acid) and Polyurethane Nanofibers Fabricated by Solution Blow Spinning as Potential Substrates for Cardiac Cell Culture. *Mater. Sci. Eng. C* **2017**, *75*, 305–316. [CrossRef] [PubMed]

43. Asaduzzaman, F.; Salmon, S. Enzyme Immobilization: Polymer–Solvent–Enzyme Compatibility. *Mol. Syst. Des. Eng.* **2022**, *7*, 1385–1414. [CrossRef]

44. Shen, J.; Yuan, Y.; Salmon, S. Carbonic Anhydrase Immobilized on Textile Structured Packing Using Chitosan Entrapment for CO 2 Capture. *ACS Sustain. Chem. Eng.* **2022**, *10*, 7772–7785. [CrossRef]

45. Pereira, A.D.S.; Diniz, M.M.; De Jong, G.; Gama Filho, H.S.; dos Anjos, M.J.; Finotelli, P.V.; Fontes-Sant'Ana, G.C.; Amaral, P.F.F. Chitosan-Alginate Beads as Encapsulating Agents for Yarrowia Lipolytica Lipase: Morphological, Physico-Chemical and Kinetic Characteristics. *Int. J. Biol. Macromol.* **2019**, *139*, 621–630. [CrossRef]

46. Festag, R.; Alexandratos, S.D.; Joy, D.C.; Wunderlich, B.; Annis, B.; Cook, K.D. Effects of Molecular Entanglements during Electrospray of High Molecular Weight Polymers. *J. Am. Soc. Mass Spectrom.* **1998**, *9*, 299–304. [CrossRef]

47. Annabi, N.; Fathi, A.; Mithieux, S.M.; Weiss, A.S.; Dehghani, F. Fabrication of Porous PCL/Elastin Composite Scaffolds for Tissue Engineering Applications. *J. Supercrit. Fluids* **2011**, *59*, 157–167. [CrossRef]

48. Janarthanan, G.; Kim, I.G.; Chung, E.J.; Noh, I. Comparative Studies on Thin Polycaprolactone-Tricalcium Phosphate Composite Scaffolds and Its Interaction with Mesenchymal Stem Cells. *Biomater. Res.* **2019**, *23*, 1. [CrossRef]

49. Islam, M.M.; Zaman, A.; Islam, M.S.; Khan, M.A.; Rahman, M.M. Physico-Chemical Characteristics of Gamma-Irradiated Gelatin. *Prog. Biomater.* **2014**, *3*, 21. [CrossRef]

50. Arjunan, P.; Umland, T.; Dyda, F.; Swaminathan, S.; Furey, W.; Sax, M.; Farrenkopf, B.; Gao, Y.; Zhang, D.; Jordan, F. Crystal Structure of the Thiamin Diphosphate-Dependent Enzyme Pyruvate Decarboxylase from the Yeast Saccharomyces Cerevisiae at 2.3 Å Resolution. *J. Mol. Biol.* **1996**, *256*, 590–600. [CrossRef]

51. Pelton, J.T.; McLean, L.R. Spectroscopic Methods for Analysis of Protein Secondary Structure. *Anal. Biochem.* **2000**, *277*, 167–176. [CrossRef] [PubMed]

52. Sóti, P.L.; Weiser, D.; Vigh, T.; Nagy, Z.K.; Poppe, L.; Marosi, G. Electrospun Polylactic Acid and Polyvinyl Alcohol Fibers as Efficient and Stable Nanomaterials for Immobilization of Lipases. *Bioprocess Biosyst. Eng.* **2016**, *39*, 449–459. [CrossRef] [PubMed]

53. Cabrera-Padilla, R.Y.; Lisboa, M.C.; Fricks, A.T.; Franceschi, E.; Lima, A.S.; Silva, D.P.; Soares, C.M.F. Immobilization of Candida Rugosa Lipase on Poly(3-Hydroxybutyrate-Co-Hydroxyvalerate): A New Eco-Friendly Support. *J. Ind. Microbiol. Biotechnol.* **2012**, *39*, 289–298. [CrossRef] [PubMed]

54. Kim, M.; Park, J.-M.; Um, H.-J.; Lee, D.-H.; Lee, K.-H.; Kobayashi, F.; Iwasaka, Y.; Hong, C.-S.; Min, J.; Kim, Y.-H. Immobilization of Cross-Linked Lipase Aggregates onto Magnetic Beads for Enzymatic Degradation of Polycaprolactone. *J. Basic Microbiol.* **2010**, *50*, 218–226. [CrossRef]